

COMBINED NATURAL CONVECTION AND SURFACE RADIATION IN A SQUARE CAVITY WITH THE INVERSELY LINEARLY HEATED OPPOSITE SIDE WALLS

Ravi Shankar Prasad^{a,*}, Ujjwal Kumar Nayak^a, Rajen Kumar Nayak^a, Amit Kumar Gupta^b

^a Department of Mechanical Engineering, B.I.T. Sindri, P.O.: Sindri Institute, Sindri, Dhanbad, Jharkhand, PIN: 828123, India

^b Department of Chemical Engineering, B.I.T. Sindri, P.O.: Sindri Institute, Sindri, Dhanbad, Jharkhand, PIN: 828123, India

ABSTRACT

This paper presents the results of numerical analysis of coupled laminar natural convection and surface radiation in a two-dimensional closed square cavity with the inversely linearly heated vertical opposite side walls and the adiabatic top and bottom walls. The cavity is filled with natural air ($Pr = 0.70$) as the fluid medium. In the present study, the governing equations i.e., Navier-Stokes Equation in the stream function - vorticity form and Energy Equation are solved for a constant property fluid under the Boussinesq approximation. For discretization of these equations, the finite volume technique is used. For the radiation calculations, the radiosity-irradiation formulation is used and the shape factors are calculated using the Hottel's crossed-string method. The effects of pertinent parameters like Rayleigh Number ($10^3 \leq Ra \leq 10^6$) and the surface emissivity of walls ($0.05 \leq \epsilon \leq 0.85$) are studied and analyzed.

Keywords: natural convection, surface radiation, stream function, vorticity, inversely linearly heated, closed cavities.

1. INTRODUCTION

In the modern times, several researchers and industrial scientists have studied combined natural convection and surface radiation heat transfer in the closed and open cavities of different geometries. The prime reasons attributed for it is its important role of in several engineering and practical science problems. Natural convection is involved with the several engineering applications like air conditioning and refrigeration, chemical and metallurgical engineering, chemical and biological warfare, food processing industries, fire control engineering, meteorological predictions, ocean engineering, solar energy, etc. Due to its inherent simplicity, reliability, quiet operation and economy, the natural convection is preferred choice for the heat dissipation and cooling. In most of such problems, the heat sources are assumed either having a constant temperature or generating heat at a constant rate for the sake of simplicity and convenience. This is quite an idealistic and unrealistic approach from the practical point of view. In most of the cases of practical problems, the heat sources may have varying temperature with the different temperature profiles. The linearly varying temperature is one of the cases, which resembles a very close approximation to the several practical situations. Studying the effect of linearly varying temperature and other parameters in natural convection coupled with surface radiation in a closed cavity is one of the realistic problems of practical importance, which needs to be analyzed in detail for the better understanding of its mechanism.

Jones and Ingham (1993) analyzed the combined convection flow in a vertical duct with linearly varying wall temperatures with depth. Singh and Venkateshan (2004) made the numerical studies of natural convection with surface radiation in side-vented open cavities. Prud'homme and Bougherara (2005) analyzed the weak non-linear

stability of stratified natural convection in a vertical cavity with lateral temperature gradient. Bouafia and Daube (2007) studied the natural convection for large temperature gradients around a square solid body within a rectangular cavity. Sathiyamoorthy *et al.* (2007a) studied the effect of the temperature difference aspect ratio on natural convection in a square cavity for nonuniform thermal boundary conditions. Sathiyamoorthy *et al.* (2007b) performed a numerical investigation of steady natural convection flows in a square cavity with the linearly heated side wall(s). Sathiyamoorthy *et al.* (2007c) studied the steady natural convection flow in a square cavity filled with a porous medium for the linearly heated side wall(s). Singh (2008) performed a numerical study of combined natural convection, conduction and surface radiation heat transfer in open top, side vented cavities. Basak *et al.* (2009a) made an analysis of mixed convection flows within a square cavity with linearly heated side wall(s). Basak *et al.* (2009b) made a natural convection flow simulation for various angles in a trapezoidal enclosure with the linearly heated side wall(s). Basak *et al.* (2010) analyzed mixed convection in a lid-driven porous square cavity with linearly heated side wall(s). Hasan *et al.* (2012) made an analysis of unsteady natural convection within a differentially heated enclosure of sinusoidal corrugated side walls. Kefayati *et al.* (2012) made a Lattice Boltzmann simulation of MHD mixed convection in a lid-driven square cavity with linearly heated wall. Basak *et al.* (2013) studied the effect of various orientations on natural convection in tilted isosceles triangular enclosures with the linearly heated inclined walls. Saravanan and Sivaraj (2015) analyzed the combined natural convection and thermal radiation in a square cavity with a non-uniformly heated plate.

Singh and Singh (2015) analyzed conjugate free convection with surface radiation in open top cavity. Karatas and Derbentli (2018) studied natural convection and radiation in rectangular cavities with one active vertical wall. Prasad *et al.* (2018a) proposed a systematic approach for

* Department of Mechanical Engineering, B.I.T. Sindri, P.O.: Sindri Institute, Sindri, Dhanbad, Jharkhand, PIN: 828123, India

† Corresponding author. Email: rsprasad.me@bitsindri.ac.in

optimal positioning of heated side walls in a side vented open cavity under natural convection and surface radiation. Prasad *et al.* (2018b) made a numerical investigation of coupled laminar natural convection and surface radiation in partially right side open cavities. Sankar *et al.* (2018) analyzed natural convection in a linearly heated vertical porous annulus. The influence of linear thermal conditions on the buoyancy driven convection in an upright porous annular space is discussed. Prasad *et al.* (2019) analyzed combined laminar natural convection and surface radiation in top open cavities with right side opening. Şahin (2020) studied the effects of the center of linear heating position on natural convection and entropy generation in a linearly heated square cavity. Kumar and Kunjuni (2021) discussed the effect of linearly varying heating inside a square cavity under natural convection with the view of thermal management of electronic and telecommunication devices.

On analysis of the literature of heat and mass transfer, there is lack of research paper discussing numerical or experimental results of natural convection and surface radiation inside the cavity having the inversely linearly heated walls. Analysis of different types of temperature distribution and heat sources provides an insight to understand the mechanism of natural convection in a better convincing way, which is helpful in analyzing the different practical situations arising with a number of heat sources or extended heat source with varying temperature in a confined area.

2. MATHEMATICAL FORMULATION

2.1 Formulation of Natural Convection

The two-dimensional steady incompressible laminar natural convection heat transfer in a closed rectangular cavity having height 'H' and horizontal width 'd' is considered. Here, the Cartesian co-ordinate system is used as shown in Fig. 1.

For a constant thermophysical property fluid under the Boussinesq approximation, the governing equations in stream function (ψ) - vorticity (ω) form, in the non-dimensional form are:

$$U \frac{\partial \omega}{\partial X} + V \frac{\partial \omega}{\partial Y} = Pr \left[\frac{\partial^2 \omega}{\partial X^2} + \frac{\partial^2 \omega}{\partial Y^2} \right] - Ra \frac{\partial \theta}{\partial Y} \quad (1)$$

$$\frac{\partial^2 \psi}{\partial X^2} + \frac{\partial^2 \psi}{\partial Y^2} = -Pr \cdot \omega \quad (2)$$

$$U \frac{\partial \theta}{\partial X} + V \frac{\partial \theta}{\partial Y} = \frac{\partial^2 \theta}{\partial X^2} + \frac{\partial^2 \theta}{\partial Y^2} \quad (3)$$

where $U = \frac{\partial \psi}{\partial Y}$, $V = -\frac{\partial \psi}{\partial X}$ and $\omega = \frac{\partial V}{\partial X} - \frac{\partial U}{\partial Y}$

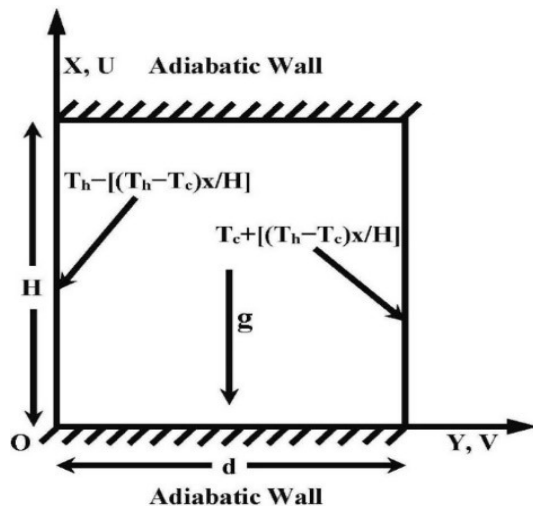


Fig. 1 Schematic diagram of problem geometry showing the computational domain

2.2 Formulation for Surface Radiation

The radiosity-irradiation formulation is used to describe the surface radiation (Singh and Venkateshan, 2004). The walls are assumed to be diffuse and gray i.e. independent of direction and wavelength.

For an elemental area on the boundary of the cavity, the non-dimensional radiosity is given by the following equation.

$$J_i = \epsilon_i (T_i/T_h)^4 + (1 - \epsilon_i) \sum_{j=1}^{2(m+n-2)} F_{ij} J_j \quad \text{where } i = 1, 2(m+n-2) \quad (4)$$

Here the view factors F_{ij} are calculated using the Hottel's crossed string method.

2.3 Boundary Conditions

The boundary condition for the computational domain enclosed by the cavity is specified in terms of non-dimensional stream function, vorticity and temperature based on the Balaji and Venkateshan (1994a, 1994b) and Sathiyamoorthy *et al.* (2007b). The boundary conditions are written here in terms of the velocities U and V also for the clarity and simplicity only.

2.3.1 Boundary Condition for Left Side Linearly Heated Wall

For the case of left side linearly heated wall:

$$T_x = T_h - [(T_h - T_c)x/H] \quad (5)$$

$$\text{Hence, } \theta = \frac{T_x - T_c}{T_h - T_c} = 1 - \frac{x}{H} = 1 - \frac{x}{d} = 1 - X \quad (6)$$

[Since for a square cavity, A=1, H = d]

Thus, the boundary condition for the left side linearly heated wall is,

$$0 < X < A, \quad Y = 0, \quad U = 0, V = 0, \text{ or } \psi = 0, \quad \omega = -\frac{1}{Pr} \frac{\partial^2 \psi}{\partial Y^2} \quad \theta = 1 - X \quad (7)$$

2.3.2 Boundary Condition for Bottom Adiabatic Wall

At the adiabatic walls, the convection and radiation energy transfer balance each other.

$$\text{Hence for the bottom adiabatic wall, } -\frac{\partial \theta}{\partial X} = N_{rc}(J-G) \quad (8)$$

Thus, the boundary conditions for the top adiabatic wall is,

$$X = 0, \quad 0 < Y < 1, \quad U = 0, V = 0, \text{ or } \psi = 0, \quad \omega = -\frac{1}{Pr} \frac{\partial^2 \psi}{\partial X^2} \quad -\frac{\partial \theta}{\partial X} = N_{rc}(J-G) \quad (9)$$

2.3.3 Boundary condition for right side wall

For the inversely linearly heated right side wall:

$$T_x = T_c + [(T_h - T_c)x/H] \quad (10)$$

$$\text{Hence, } \theta = \frac{T_x - T_c}{T_h - T_c} = \frac{x}{H} = \frac{x}{d} = X \quad (11)$$

[Since for a square cavity, A=1, H = d]

Thus, the boundary condition for the right side inversely linearly heated wall is,

$$0 < X < A, \quad Y = 1, \quad U = 0, V = 0, \text{ or } \psi = 0, \quad \omega = -\frac{1}{Pr} \frac{\partial^2 \psi}{\partial Y^2} \quad \theta = X \quad (12)$$

2.3.4 Boundary condition for top adiabatic wall

At the adiabatic walls, the convection and radiation energy transfer balance each other.

$$\text{Hence for the top adiabatic wall, } \frac{\partial \theta}{\partial X} = N_{rc}(J-G) \quad (13)$$

Thus, the boundary condition for the top adiabatic wall is,

$$X = A, \quad 0 < Y < 1, \quad U = 0, V = 0, \text{ or } \psi = 0, \quad \omega = -\frac{1}{Pr} \frac{\partial^2 \psi}{\partial X^2} \quad \frac{\partial \theta}{\partial X} = N_{rc}(J-G) \quad (14)$$

3. METHOD OF SOLUTION

The governing equations (1), (2) and (3) are transformed into finite difference equations using the finite volume based finite difference method. Then the Gauss-Seidel iterative procedure is used to solve the algebraic equations obtained. A computer code for a FORTRAN platform is developed for solving the discretized equations. An optimum grid size of 41x41 is selected for the computational domain on the basis of grid sensitivity analysis (as suggested by Singh and Venkateshan, 2004). A cosine function has been chosen to generate the grids along both the X and Y directions in computational domain of the closed cavity. These cosine grids are very fine near the solid boundaries, where the gradients are very steep, while they are relatively coarser in the remaining part of the domain as shown in Fig. 2. Derivative boundary conditions are implemented by three-point formulae using the Lagrangian polynomial. The integration required in calculations is performed by using the Simpson's one-third rule for the non-uniform step size. Upwinding has been used for representing the advection terms to ensure the stable and convergent solutions. Under relaxation with a relaxation parameter 0.1 is used for all the equations except for the radiosity equations, where the relaxation parameter 0.5 is used.

A convergence criterion (δ) in the percentage form has been defined as

$$\delta = \left| (\zeta_{new} - \zeta_{old}) / \zeta_{new} \right| \times 100 \quad (15)$$

where ζ is any dependent variable like ψ , ω , θ , J and G , over which the convergence test is applied. Here the subscripts "old" and "new" refers to the first and second values of ζ calculated in the any two successive iterations. A convergence criterion of 0.01% or 10^{-4} has been used for stream function, vorticity and temperature, whereas the convergence criterion of 0.001% or 10^{-5} has been used for the radiosity.

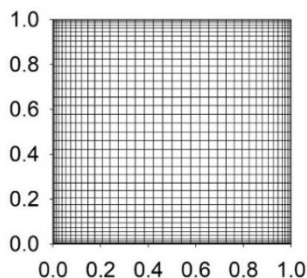


Fig. 2 Typical grid patterns used in the analysis. A=1, Grid size = 41x41.

4. RESULTS AND DISCUSSION

The Table 1 shows the range of parameters considered in the present study. The results are presented with the objective of analytical comparison between the different cases considered. A grid sensitivity study is performed for the determination of optimum grid size for the present study.

Table 1 Range of parameters considered for the present study

Parameters	Range
Rayleigh Number, Ra_H	10^3 - 10^6
Conduction-radiation parameter, N_{re}	42.261
Emissivity, ϵ	0.05-0.85
Aspect Ratio, A	1.0

4.1 Grid Sensitivity Study

A grid sensitivity study or grid independence study based on \overline{Nu}_C , \overline{Nu}_R and \overline{Nu}_T is performed to find the optimum grid size as suggested by Singh and Venkateshan (2004). On the basis of this grid independence test a grid size 41x41 is found to be optimum for the present problem.

Any further increase in the grid size increases the computational work manifolds without more significant improvement in the accuracy of results.

4.2 Validation

There is a lack of experimental results for the cavities having linearly heated side walls in the similar cases and only a few numerical results are available in the similar cases for comparison. For validation, the results obtained using the present code are compared with the numerical results of Sathiyamoorthy *et al.* (2007b) under the identical boundary conditions. There a very good agreement is observed between the streamlines and isotherms using the present code and in the results of Sathiyamoorthy *et al.* (2007b) under the identical boundary conditions.

4.2.1 Comparison with Sathiyamoorthy *et al.* (2007b)

For validation, comparing with the results of the of Sathiyamoorthy *et al.* (2007b), a very good agreement is observed between the results of both sides identical linearly heated wall and the results of Sathiyamoorthy *et al.* (2007b) under identical boundary conditions. At the lower Rayleigh number, the results of the two studies are almost identical. At the higher Rayleigh number also, the two results agree qualitatively. But at the higher Rayleigh numbers, there some marked differences in the streamlines and the isotherms as well as the local Nu_C at the bottom wall and the linearly heated side walls exist. There in the results by Sathiyamoorthy *et al.* (2007b), the surface radiation is not taken into account. Due to lack of experimental results for the cavity having linearly heated side walls, the results of the present study cannot be verified independently. However, these differences in the results at the higher Rayleigh number needs to be further investigated by the other experimental and numerical methods.

4.3 Analysis of Natural Convection in a Square Cavity having left and right inversely linearly heated left and right side wall

In this case, there is bottom adiabatic wall, left side linearly heated wall with hot at bottom and cold at top, top adiabatic wall and right side inversely linearly heated wall with cold at bottom and hot at top.

4.3.1 Variation of Streamlines with Rayleigh Number

Fig. 3 shows the streamline inside the cavity at the different Rayleigh number. Here the streamlines in the cavity shows formation of the two separate rolls in the cavity. These two air circulation loops exist in the upper and lower halves of the cavity. There is the less interaction of fluids between the two circulation loops in the cavity.

Here, the negative and positive signs of stream functions show the anticlockwise and clockwise circulations of air in the cavity respectively.

There for the top circulation loop, the heat source is at the right and the heat sink exists in the left. Thus, the air becomes hot at the right, raises in the upward direction turns to the left along the top adiabatic wall and comes down along the cold left wall. Thus, the circulation in the top half of the cavity exist in the anticlockwise direction.

There for the bottom circulation loop, the heat source is at the left and heat sink exists in the right. Thus, the air becomes hot at the left, raises in the upward direction turns to the right at the mid of the cavity and comes down along the cold right wall. Thus, the circulation in the bottom half of the cavity exist in the clockwise direction.

The direction of air velocity in the two circulation loops agrees at the mid horizontal plane of the cavity and it is from left to right. The two circulation loops divide the cavity virtually in two parts i.e., the top and the bottom part. The results may be useful in the design of food storage, refrigerator, cold storage etc. as there non-mixing of odors or air in the different parts or compartments is sought.

The increased air circulation inside the cavity with the increased Rayleigh number is observed. However, the basic airflow pattern inside the cavity remains unaffected with the increased Rayleigh number.

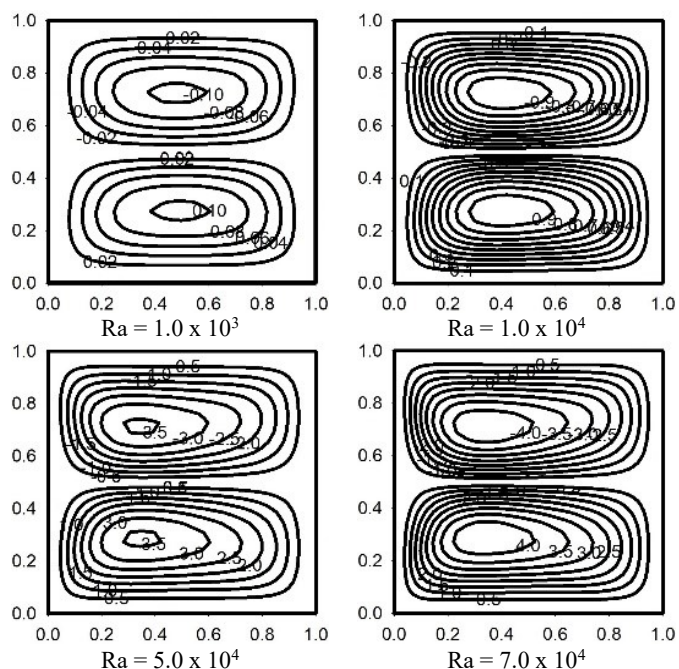


Fig. 3 Variation of streamlines with Rayleigh number for $A = 1.0$, $Pr = 0.70$.

4.3.2 Variation of Isotherms with Rayleigh Number

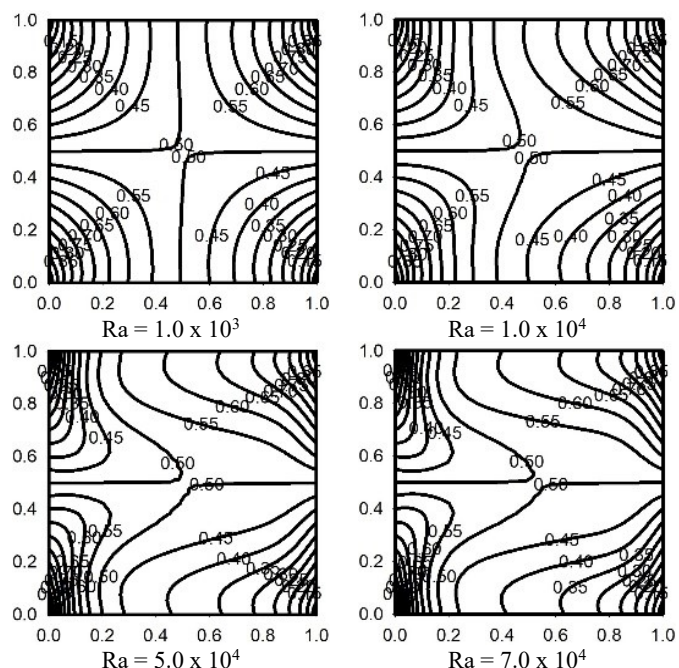


Fig. 4 Variation of isotherms with Rayleigh number for $A = 1.0$, $Pr = 0.70$.

Fig. 4 shows the isotherms inside the cavity at the different Rayleigh number. It is observed that the temperature at the middle part of the cavity remains close to the average temperature of the linearly heated side wall. It is observed that at the lower Rayleigh number, the isotherms are straight and conduction dominates in the cavity. At the higher Rayleigh numbers, the isotherms get curved showing the increased buoyancy forces in the cavity. At the higher Rayleigh numbers, the natural convection is the dominant mode of heat transfer and a dense isotherms are observed close to the top and bottom ends of left linearly heated side walls. This shows relatively better cooling of left side bottom wall. The presence of two straight horizontal isotherms at the mid horizontal section is an evidence of formation of two circulation loops at the top and

bottom halves of the cavity separated at the mid horizontal section as shown in Fig. 3.

4.3.3 Variation of Isotherms with Rayleigh Number

Fig. 5 shows the variation of non-dimensional temperature along the horizontal width at the three horizontal sections i.e. at the bottom horizontal section ($X = 0$), the mid horizontal section ($X = 0.5$) and the top horizontal section ($X = 1.0$). At the bottom wall of the cavity, the temperature varies from 1.0 at the left to 0 at the right. At the mid horizontal section of the cavity, the temperature is almost constant at the temperature close to the mean temperature of linearly heated side walls i.e., 0.50. This is the temperature of the air stream moving from left to right at the middle section of the cavity. At the top wall of the cavity, the temperature varies from 0 at the left to 1.0 at the right.

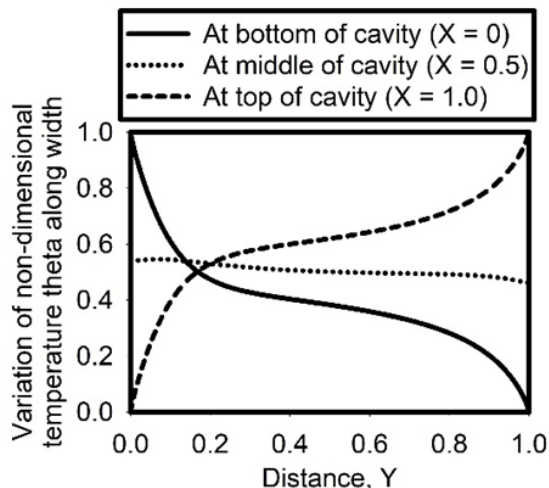


Fig. 5 Variation of non-dimensional temperature along horizontal width at the different horizontal sections for $A = 1.0$, $Pr = 0.70$, $Ra = 7.0 \times 10^7$.

4.3.4 Variation of local Nuc at left side linearly heated wall with Rayleigh number

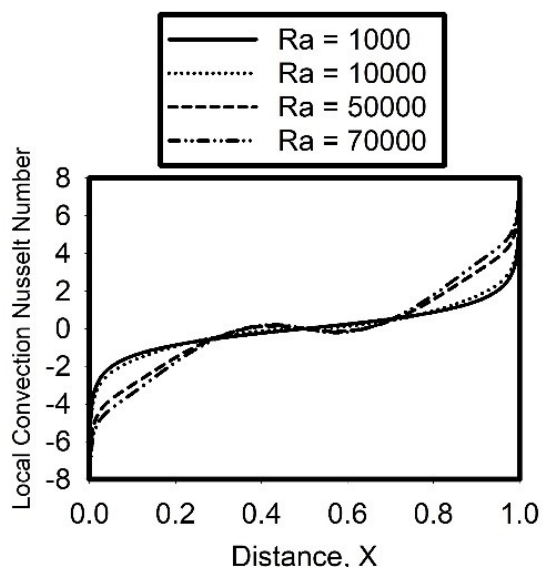


Fig. 6 Variation of local Nu_C at linearly heated left side wall along height with Rayleigh number for $A = 1$, $Pr = 0.70$.

Fig. 6 shows the variation of local convection Nusselt number (dimensionless temperature gradient in the perpendicular direction) at the left side linearly heated wall at the different Rayleigh numbers. Here at

the left side linearly heated wall, the local convection Nusselt number varies from negative at the bottom to positive at the top. This shows that the bottom hot part of the left wall is losing heat and the top cold part of the left wall is gaining heat. At the higher Rayleigh number, the increased buoyant forces and increased convective currents causes the fluctuations in the local convection Nusselt number at the left side linearly heated wall.

4.3.5 Variation of local Nu_C at right side inversely linearly heated wall with Rayleigh number

Fig. 7 shows the variation of local convection Nusselt number (dimensionless temperature gradient in the perpendicular direction) at the right side inversely linearly heated wall at the different Rayleigh numbers. Here at the right side inversely linearly heated wall the local convection Nusselt number varies from positive at the bottom to negative at the top. This shows that the bottom cold part of the right wall is gaining heat and the top hot part of the right wall is losing heat. At the higher Rayleigh number, the increased buoyant forces and increased convective currents causes the fluctuations in the local convection Nusselt number at the right side inversely linearly heated wall.

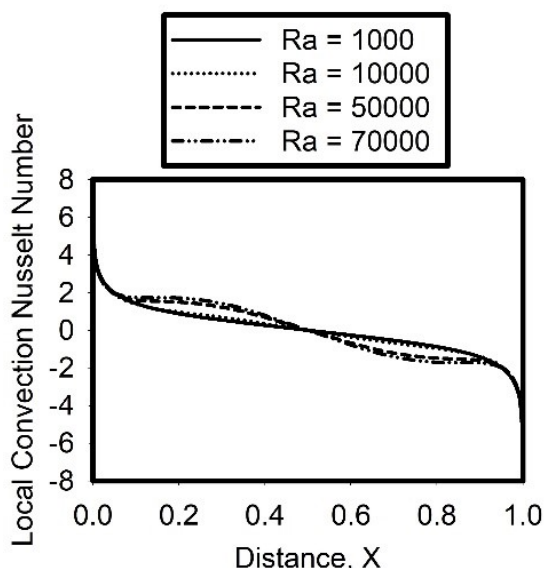


Fig. 7 Variation of local Nu_C at inversely linearly heated right side wall along height with Rayleigh number for $A = 1.0$, $Pr = 0.70$.

4.4 General Discussion

From the present study, the following observations are made.

1. In a closed cavity having linearly heated side walls, the fluid circulations primarily depend upon the Rayleigh number.
2. At the lower Rayleigh number, only the conduction is the dominant mode of heat transfer.
3. At the higher Rayleigh number, the primary air circulation becomes stronger. In this case, some small secondary air circulations may grow along with the strong primary air circulations enhancing the mixing of fluids.
4. At the higher Rayleigh number, the heat transfer by the natural convection increases in all the cases.
5. The local Nu_C at the linearly heated side walls at the higher Rayleigh number at the lower portion of walls shows the interaction with the strong primary and secondary air circulations.
6. In the case of the two inversely linearly heated left and right side walls, there are two circulation loops at the lower and upper halves of the cavity.
7. The thermal interaction at the left side wall is slightly better due to hot part of wall at the bottom.
8. The temperature of the major part of the cavity is close to the mean temperature of the linearly heated wall.

5. CONCLUSIONS

The natural convection in a closed cavity highly depends on Rayleigh number. With the increase in Rayleigh number, the air circulation in the cavity increases affecting the results like streamlines, isotherms and variation in local Nu_C at the linearly heated vertical side wall(s). The local Nusselt number at the linearly heated side wall is changing with the increase in Rayleigh number due to interaction of primary and secondary air circulation loops with the linearly heated walls. In the case of two inversely linearly heated wall, the two primary air circulation loops are observed in the vertical plane. These linearly heated wall has a great impact on the natural convection air currents in the cavity.

The results of present study have a very good agreement with other numerical results under identical conditions. At the higher Rayleigh number, the two results agree qualitatively. However, there several marked differences also exist, which need to be verified by the other experimental and numerical methods.

NOMENCLATURE

A	aspect ratio = H/d
d	spacing between left and right walls, m
$F_{i,j}$	view factor or shape factor between the elements i and j
g	acceleration due to gravity, 9.81 m.s^{-2}
G	dimensionless elemental irradiation
Gr_H	Grashof Number based on H $= g\beta(T_h - T_\infty)H^3/\nu^2$
H	height of the cavity, m
J	dimensionless elemental radiosity
m	total number of grid points in horizontal Y direction in the computational domain
n	total number of grid points in vertical X direction in the computational domain
N_{rc}	radiation-conduction parameter
Nu_C	convection Nusselt number
$\overline{Nu_C}$	average convection Nusselt number
Pr	Prandtl number
Ra_H	Rayleigh number based on H
T	temperature, K
T_x	temperature of left or right wall at a point having height x or having X -coordinate x , K
T_h	temperature of the hot wall of cavity, K
T_R	temperature ratio = T_∞ / T_h
T_∞	temperature of the ambient, K
U	dimensionless vertical velocity
V	dimensionless horizontal velocity
X	dimensionless vertical coordinate = x/d
Y	dimensionless horizontal coordinate = y/d

Greek Symbols

α	thermal diffusivity of fluid, $\text{m}^2.\text{s}^{-1}$
β	isobaric co-efficient of volumetric thermal expansion of fluid, K^{-1}
δ	convergence parameter in percentage $= (\zeta_{\text{new}} - \zeta_{\text{old}}) / \zeta_{\text{new}} \times 100$
ϵ	emissivity of the walls
ζ	symbol for the any dependent variable ($\psi, \omega, \theta, J, G$) over which convergence test is being applied
θ	dimensionless temperature $= (T - T_\infty) / (T_h - T_\infty)$
ν	kinematic viscosity of the fluid, $\text{m}^2.\text{s}^{-1}$
σ	Stefan Boltzmann constant, $5.67 \times 10^{-8} \text{ W.m}^{-2}.\text{K}^{-4}$
ψ	dimensionless stream function
ω	dimensionless vorticity

Subscripts

c	cold
C	convection
h	hot
H	based on the height H of the left wall of closed cavity
i	any arbitrary elemental area of an enclosure in horizontal direction
j	any arbitrary elemental area of an enclosure in vertical direction
new	present value of any dependent variable ($\psi, \omega, \theta, J, G$) obtained in two successive iteration
old	previous value of any dependent variable ($\psi, \omega, \theta, J, G$) obtained in two successive iteration
rc	radiation-conduction
R	radiation
∞	ambient

REFERENCES

- Balaji, C., and Venkateshan, S.P., 1994a, "Correlations for free convection and surface radiation in a square cavity," *International Journal of Heat and Fluid Flow*, **15**(3), 249-251.
[https://dx.doi.org/10.1016/0142-727X\(94\)90046-9](https://dx.doi.org/10.1016/0142-727X(94)90046-9)
- Balaji, C., and Venkateshan, S.P., 1994b, "Interaction of radiation with free convection in an open cavity," *International Journal of Heat and Fluid Flow*, **15**(4), 317-324.
[https://dx.doi.org/10.1016/0142-727X\(94\)90017-5](https://dx.doi.org/10.1016/0142-727X(94)90017-5)
- Basak, T., Roy, S., Sharma, P.K., and Pop, I., 2009a, "Analysis of mixed convection flows within a square cavity with linearly heated side wall(s)," *International Journal of Heat and Mass Transfer*, **52**(9-10), 2224-2242.
<https://dx.doi.org/10.1016/j.ijheatmasstransfer.2008.10.033>
- Basak, T., Roy, S., Singh, A., and Pandey, B.D., 2009b, "Natural convection flow simulation for various angles in a trapezoidal enclosure with linearly heated side wall(s)," *International Journal of Heat and Mass Transfer*, **52**(19-20), 4413-4425.
<https://dx.doi.org/10.1016/j.ijheatmasstransfer.2009.03.057>
- Basak, T., Roy, S., Singh, S.K., and Pop, I., 2010, "Analysis of mixed convection in a lid-driven porous square cavity with linearly heated side wall(s)," *International Journal of Heat and Mass Transfer*, **53**(9-10), 1819-1840.
<https://dx.doi.org/10.1016/j.ijheatmasstransfer.2010.01.007>
- Basak, T., Anandalakshmi, R., and Roy, M., 2013, "Heatlines based natural convection analysis in tilted isosceles triangular enclosures with linearly heated inclined walls: Effect of various orientations," *International Communications in Heat and Mass Transfer*, **43**, 39-45.
<https://dx.doi.org/10.1016/j.icheatmasstransfer.2013.01.008>
- Bouafia, M., and Daube, O., 2007, "Natural convection for large temperature gradients around a square solid body within a rectangular cavity," *International Journal of Heat and Mass Transfer*, **50**(17-18), 3599-3615.
<https://dx.doi.org/10.1016/j.ijheatmasstransfer.2006.05.013>
- Hasan, M.N., Saha, S.C., and Gu, Y.T., 2012, "Unsteady natural convection within a differentially heated enclosure of sinusoidal corrugated side walls," *International Journal of Heat and Mass Transfer*, **55**(21-22), 5696-5708.
<https://dx.doi.org/10.1016/j.ijheatmasstransfer.2012.05.065>
- Jones, A.T., and Ingham, D.B., 1993, "Combined convection flow in a vertical duct with wall temperatures that vary linearly with depth," *International Journal of Heat and Fluid Flow*, **14**(1), 37-47.
[https://dx.doi.org/10.1016/0142-727X\(93\)90038-O](https://dx.doi.org/10.1016/0142-727X(93)90038-O)
- Karatas, H., and Derbentli, T., 2018, "Natural convection and radiation in rectangular cavities with one active vertical wall," *International Journal of Thermal Sciences*, **123**, 129-139.
<https://dx.doi.org/10.1016/j.ijthermalsci.2017.09.006>
- Kefayati, G.R., Gorji-Bandpy, M., Sajjadi, H., and Ganji, D.D., 2012, "Lattice Boltzmann simulation of MHD mixed convection in a lid-driven square cavity with linearly heated wall," *Scientia Iranica*, **19**(4), 1053-1065.
<https://dx.doi.org/10.1016/j.scient.2012.06.015>
- Kumar, R.A., and Kunjunni, M., 2021, "Effect of linearly varying heating inside a square cavity under natural convection," *Journal of Applied research and Technology*, **19**(4), 336-344.
<https://doi.org/10.22201/icat.24486736e.2021.19.4.1573>
- Prasad, R.S., Singh, S.N., and Gupta, A.K., 2018a, "A systematic approach for optimal positioning of heated side walls in a side vented open cavity under natural convection and surface radiation," *Frontiers in Heat and Mass Transfer*, **11**, 15.
<https://dx.doi.org/10.5098/hmt.11.15>
- Prasad, R.S., Singh, S.N., and Gupta, A.K., 2018b, "Coupled laminar natural convection and surface radiation in partially right side open cavities," *Frontiers in Heat and Mass Transfer*, **11**, 28.
<https://dx.doi.org/10.5098/hmt.11.28>
- Prasad, R.S.; Singh, S.N. and Gupta, A.K., 2019, "Combined laminar natural convection and surface radiation in top open cavities with right side opening," *Journal of Engineering Science and Technology*, **14**(1), 387-410.
https://jestec.taylors.edu.my/Vol%2014%20issue%201%20February%202019/14_1_27.pdf
(Last accessed on 25th February, 2022)
- Prud'homme, M., and Bougherara, H., 2005, "Weakly non-linear stability of stratified natural convection in a vertical cavity with lateral temperature gradient," *International Communications in Heat and Mass Transfer*, **32**(1-2), 32-42.
<https://dx.doi.org/10.1016/j.icheatmasstransfer.2004.02.020>
- Şahin, B., 2020, "Effects of the center of linear heating position on natural convection and entropy generation in a linearly heated square cavity," *International Communications in Heat and Mass Transfer*, **117**, 104675.
<https://dx.doi.org/10.1016/j.icheatmasstransfer.2020.104675>
- Sankar, M., Kiran, S., and Sivasankaran, S., 2018, "Natural convection in a linearly heated vertical porous annulus," *Journal of Physics: Conference Series*, **1139**, 012018.
<https://dx.doi.org/10.1088/1742-6596/1139/1/012018>
- Saravanan, S., and Sivaraj, C., 2015, "Combined natural convection and thermal radiation in a square cavity with a non-uniformly heated plate," *Computers & Fluids*, **117**, 125-138.
<https://dx.doi.org/10.1016/j.compfluid.2015.05.005>
- Sathiyamoorthy, M., Basak, T., Roy, S., and Mahanti, N.C., 2007a, "Effect of the temperature difference aspect ratio on natural convection in a square cavity for nonuniform thermal boundary conditions," *Journal of Heat Transfer*, **129**(12), 1723-1728.
<https://dx.doi.org/10.1115/1.2768099>
- Sathiyamoorthy, M., Basak, T., Roy, S., and Pop, I., 2007b, "Steady natural convection flows in a square cavity with linearly heated side wall(s)," *International Journal of Heat and Mass Transfer*, **50**(3-4), 766-775.
<https://dx.doi.org/10.1016/j.ijheatmasstransfer.2006.06.019>

Sathiyamoorthy, M., Basak, T., Roy, S., and Pop, I., 2007c, "Steady natural convection flow in a square cavity filled with a porous medium for linearly heated side wall(s)," *International Journal of Heat and Mass Transfer*, **50**(9–10), 1892-1901.
<https://dx.doi.org/10.1016/j.ijheatmasstransfer.2006.10.010>

Singh, S.N., and Venkateshan, S.P., 2004, "Numerical study of natural convection with surface radiation in side-vented open cavities," *International Journal of Thermal Sciences*, **43**(9), 865–876.
<https://dx.doi.org/10.1016/j.ijthermalsci.2004.01.002>

Singh, S.N., 2008, "Numerical study of combined natural convection, conduction and surface radiation heat transfer in open top, side vented cavities," *International Journal Heat and Technology*, **26**(2), 101-109.
<https://iieta.org/Journals/IJHT/Archive/Vol-26-No-2-2008>

Singh, D.K., and Singh, S.N., 2015, "Conjugate free convection with surface radiation in open top cavity," *International Journal of Heat and Mass Transfer*, **89**, 444-453.
<https://dx.doi.org/10.1016/j.ijheatmasstransfer.2015.05.038>